

Article

# Investigation on Fuel Properties of Synthetic Gasoline-like Fuels

Weidi Huang<sup>1,2</sup>, Koichi Kinoshita<sup>1,\*</sup>, Yohko Abe<sup>1</sup>, Mitsuharu Oguma<sup>1</sup>,  
and Kotaro Tanaka<sup>2,3</sup>

<sup>1</sup> Research Institute for Energy Conservation, National Institute of Advanced Industrial Science and Technology, 1-2-1 Namiki, Tsukuba, Ibaraki 305-8564, Japan

<sup>2</sup> Carbon Recycling Energy Research Centre, Ibaraki University, 4-12-1 Nakanarusawa, Hitachi, Ibaraki 316-8511, Japan

<sup>3</sup> Graduate School of Science and Engineering, Ibaraki University, 4-12-1 Nakanarusawa, Hitachi, Ibaraki 316-8511, Japan

\* Correspondence: koichi-kinoshita@aist.go.jp

Received: 08 November 2023; Revised: 18 February 2024; Accepted: 25 March 2024; Published: 27 March 2024

**Abstract:** Synthetic fuels have gained considerable attention due to their promising characteristics. A comprehensive survey was undertaken to assess the availability of synthetic fuels in the global market, followed by an investigation to evaluate their potential in engines. This report presents the initial findings regarding the physical and chemical properties of synthetic gasoline-like fuels, specifically DMC (dimethyl carbonate), bioethanol, EtG (ethanol-to-gasoline), G40, and bio-naphtha. A comparison was conducted between these synthetic fuels and conventional gasoline. Furthermore, discussions were provided to enhance the understanding of the potential influence of fuel properties on spray and combustion characteristics. EtG and G40 are specifically designed to emulate conventional gasoline. Results indicate that EtG and gasoline should be directly interchangeable in the engine or blended in any proportion because they have almost identical Research Octane Number (RON)/Motor Octane Number (MON), fuel density, and higher heating value (HHV). G40 has a higher RON (105) compared with that of gasoline (92.2), likely resulting from the high content of iso-paraffin in G40. Bio-naphtha exhibits the high fraction of paraffin and naphthene content relative to other fuels. The feature of chemical compositions results in a lower RON (55.9), lower HHV and smaller fuel density compared to other fuels. DMC and bioethanol blends in gasoline were investigated. Regardless of whether DMC or bioethanol is incorporated, under a 60% blend ratio, gasoline distillation accelerates initially, until DMC or bioethanol completely evaporates, after which gasoline distillation returns to its normal rate. With increasing the volumetric fraction of the ethanol in the blends, either chemical compositions or the RON/HHV basically change linearly.

**Keywords:** synthetic fuels; gasoline-like fuels; physical and chemical fuel properties; chemical compositions

## 1. Introduction

Synthetic fuels are artificial fuel sources created by utilizing carbon dioxide (CO<sub>2</sub>) and hydrogen (H<sub>2</sub>) as primary ingredients. Similar to traditional petroleum products, synthetic fuels consist of a range of hydrocarbons, allowing for customized production suited for specific uses like gasoline or kerosene. Particularly noteworthy are “e-fuels,” which are synthetic fuels derived from “green hydrogen,” produced through renewable energy sources. Several studies have demonstrated that internal combustion engine (ICE) vehicles powered by e-fuels have the potential to achieve significant reduction in CO<sub>2</sub> emission comparable those of electric vehicles (EVs) [1–3]. This is particularly significant as it allows for long-distance and heavy-duty applications, utilizing existing infrastructure, and offers energy storage solutions.



In a significant development, the European Union approved the continued use of e-fueled internal combustion engine (ICE) vehicles within the EU beyond the year 2035, as confirmed in March 2023 [4]. This approval demonstrates the EU's recognition of e-fuels as a viable solution in the ongoing efforts to decarbonize the transportation sector. Furthermore, the Japanese government is actively supporting research and development initiatives related to the production and utilization of e-fuels, emphasizing their importance [5]. These initiatives underscore the increasing global recognition of e-fuels' potential as a sustainable alternative in the transition towards cleaner transportation systems.

Synthetic fuels encompass a range of fuel types with distinct molecular structures. In a comprehensive review conducted by Ram et al. [6], synthetic fuels are categorized based on their feedstock, which includes biofuels, synthetic hydrogen fuels, gas-to-liquid (GtL) fuels, and power-to-liquid (PtL) fuels. This classification provides a comprehensive understanding of the diverse sources and production processes involved in synthetic fuel production.

Biofuels are a type of synthetic fuels derived from biological materials, such as vegetable oils, animal fats, or waste products. Among these biofuels, Hydrotreated Vegetable Oil (HVO) fuel, also referred to as renewable diesel or green diesel, is a notable example [7]. HVO is produced through the hydrotreatment process, which involves refining vegetable oils or animal fats. Another well-known biofuel is bioethanol, primarily sourced from crops with high sugar or starch content [8]. Bioethanol have also gained significant global adoption, being used either in blended forms with fossil fuels or as standalone fuels [9]. Commercial bioethanol production primarily relies on first-generation (1G) feedstocks but concerns about its competition with food raise sustainability issues. Second-generation (2G) bioethanol from lignocellulosic biomass offers a cleaner alternative, yet high production costs persist. Ongoing research focuses on addressing these challenges, analyzing economic aspects, and developing suitable methods for the large-scale commercialization of 2G bioethanol [10].

Synthetic hydrogen fuels, on the other hand, are synthetic fuels produced by combining hydrogen with other molecules, often involving carbon dioxide [11]. Methanol and DME (dimethyl ether) are common examples of synthetic hydrogen fuels created through synthetic processes involving hydrogen and carbon dioxide. It is important to note that the most prevalent source of hydrogen is derived from fossil fuels, known as grey hydrogen, which releases carbon dioxide during its production process and contributes to climate change [12]. Therefore, in the context of current industrial manufacturing, synthetic hydrogen fuels are not zero-emission fuels.

GtL fuels are synthetic fuels produced using natural gas or other gases as feedstocks. When these gases are sourced from biogas generated through the anaerobic digestion of organic matter, such as food waste or agricultural waste, GtL fuels become carbon neutral. Synthetic fuels derived from GtL feedstocks are typically produced through the Fischer-Tropsch (FT) process. FT process stands as a well-established method, proficient in converting syngas into higher hydrocarbons, particularly liquid fuels (Naphtha, kerosene, diesel, etc.) for transportation. While existing large-scale plants primarily rely on CH<sub>4</sub> reforming or coal gasification, implementing biomass-based FT facilities should encounter minimal technical hurdles. Growing environmental concerns, heightened fossil fuel usage, and technological advancements have sparked renewed interest in FT synthesis. FT fuels, when utilized in internal combustion engines, demonstrate lower emission levels compared to traditional gasoline and diesel, owing to their sulfur-free composition, minimal aromatics, and low nitrogen concentrations [13].

PtL fuels are synthetic fuels created by utilizing renewable electricity to convert water and carbon dioxide into liquid fuel through the FT route or other routes [14]. The production of PtL fuels does not result in the release of additional carbon dioxide into the atmosphere, making them an environmentally friendly alternative to synthetic hydrogen fuels. Current developments in PtL fuels involve the production of methanol, ethanol, DME, synthetic diesel, synthetic gasoline, and so forth [14]. Additionally, ammonia can be synthesized by combining nitrogen (captured from the air) with hydrogen (produced through electrolysis) and thus, it can also be classified as a PtL fuel [15].

Recent reports have highlighted the advantages of PtL fuels compared to other synthetic fuels, including reduced greenhouse gas emissions, lower water demand, and decreased land-use requirements [16]. Consequently, PtL fuels have gained significant attention as a promising area of study [17,18]. Recognizing the potential of PtL fuels, the Japanese New Energy and Industrial Technology Development Organization

(NEDO) initiated a project in 2021 [19]. This project primarily focuses on advancing the FT reaction of PtL fuels, with the goal of developing a next-generation FT process.

As part of the NEDO investigation, a comprehensive survey was conducted to assess not only PtL fuels but also other synthetic fuels available in the global market. Within this report, the preliminary findings regarding the physical and chemical properties of synthetic gasoline-like fuels are presented. The properties of fuels play a crucial role in influencing both the formation of fuel-air mixtures and the subsequent combustion processes within ICEs. On one hand, changes in fuel properties can lead to variations in needle valve movement, liquid core breakup, and spray characteristics [20–24]. Furthermore, the composition, volatility, density, viscosity, and other physical and chemical properties of fuels have a direct impact on how effectively they mix with air, the stability of the resulting mixture, and the characteristics of the combustion process [25,26]. Therefore, as the first step in the ongoing synthetic fuels investigation, the unveiling physical and chemical properties of synthetic fuels is deemed crucial.

## 2. Methods

### 2.1. Testing Fuels

This study examined the physical and chemical properties of five different types of synthetic fuels, including EtG (ethanol-to-gasoline), G40 (10% Bioethanol, 30% MtG (Methanol to gasoline), and 60% gasoline in volume fraction), bio-naphtha, DMC (dimethyl carbonate), and bioethanol, in addition to conventional gasoline. It is worth noting that among these synthetic fuels, EtG, G40, and bio-naphtha are mixtures, whereas DMC and bioethanol are pure substances.

DMC, Bioethanol, and G40 were provided by the Karlsruhe Institute of Technology. Bioethanol was derived from biomass, while DMC was synthesized from CO<sub>2</sub> and biomethanol. G40 is designed to meet the requirements of EN228 [27]. EtG and bio-naphtha were imported from Coryton Advanced Fuels Ltd. EtG was synthesized from bioethanol and is functionally equivalent to fossil-derived gasoline meeting EN228 [28]. Bio-naphtha was synthesized from biomaterial through the FT process. For comparison of fuel properties, gasoline, obtained from a domestic gas station in Japan, was also used in this study.

It is noteworthy to acknowledge that the DMC and bioethanol investigated in this study, despite being produced through a synthetic process, consist of a single component. As pure substances, their fuel properties, spray characteristics, and combustion behavior are expected to align with previous investigations [29, 30], irrespective of the specific manufacturing route. Consequently, the present study directed its analysis towards the blends of DMC and Bioethanol with domestic gasoline, exploring the effects of different volume fractions on fuel characteristics and performance. It should be explained that methanol, a crucial type of synthetic fuels, holds significance as it can be synthesized through the FT process [31]. Exploring the potential of blending methanol with gasoline or other synthetic fuels could provide valuable insights. However, it is imperative to recognize that the safety concerns associated with methanol, given its well-established toxicity, have prevented the execution of such experiments. Consequently, the experiment could not be conducted to address this research topic. The testing fuels used in the study are listed in Table 1.

**Table 1.** List of testing fuels.

| Sampling No. | Gasoline | EtG       | G40       | Bio-Naphtha | DMC Blends | Bioethanol Blends |
|--------------|----------|-----------|-----------|-------------|------------|-------------------|
| -            | [vol. %] | [vol. %]  | [vol. %]  | [vol. %]    | [vol. %]   | [vol. %]          |
| 1            | 100 (#1) | -         | -         | -           | -          | -                 |
| 2–3          | 80       | -         | -         | -           | 20 (#2)    | 20 (#3)           |
| 4–5          | 60       | -         | -         | -           | 40 (#4)    | 40 (#5)           |
| 6–7          | 40       | -         | -         | -           | 60 (#6)    | 60 (#7)           |
| 8–9          | 20       | -         | -         | -           | 80 (#8)    | 80 (#9)           |
| 10–14        | -        | 100 (#10) | 100 (#11) | 100 (#12)   | 100 (#13)  | 100 (#14)         |




## 2.2. Analyzing Measures

Three instruments were used in this study to analyze physical and chemical properties of testing fuels, as shown in Table 2. The distillation degree of the testing fuels was measured using the Automated Distillation Tester (Tanaka Scientific limited AD-6 Type). The fuel density of the testing fuels was directly measured using the Tester named Anton Paar DMA 4100M. The tester has a measuring range of 0 to 3 g/cm<sup>3</sup> with an accuracy of 0.0001 g/cm<sup>3</sup>. In this study, the fuel density of the testing fuels was measured at 15 °C. The temperature controlling accuracy of the tester is 0.03 °C.

The chemical properties of synthetic fuels were analyzed using an HP 6890 Series Gas Chromatograph (GC), and the collected data was processed on a HP ChemStation (Agilent Technologies). In the GC, the liquid fuel sample was first vaporized to convert it into a gas. The gas was then carried by a carrier gas, such as helium or nitrogen, into the GC column. The GC column used in this research was a specific type called HP-DHA1, with a diameter of 0.25 mm and a film thickness of 0.5 μm. This column was responsible for separating and analyzing the components of the vaporized fuel. As the separated components exited the column, they were detected using a Flame Ionization Detector (FID). The FID measured the concentration of each component and generated a graph known as a chromatogram. Specifically, each measured component in the sample gas will have a peak, which is the change in detector output because of the component passing over the measure detector. The controller determines which component the peak represents by the retention time, the time from the beginning of the analysis cycle to when the highest point of the peak is. By comparing the chromatogram to known standards, it was possible to identify the components present in the liquid fuel sample and determine their respective quantities. More details can refer to reference [32].

It should be clarified that each measurement was performed only once. However, the experimental results are believed to be reliable because all measurements were conducted using automated instruments, minimizing potential human error. Therefore, any measurement error is solely dependent on the precision of the instruments used. Although conducting repeated measurements at different time intervals (such as monthly or longer) may introduce some variations. These variations may be influenced by factors such as storage conditions and fluctuations in fuel supply.

**Table 2.** The instruments used for analyzing physical and chemical properties of testing fuels.

|                 |   |  |   |
|-----------------|---|--|---|
| Type            |  |  |  |
|                 | Anton Paar DMA 4100M  | Tanaka Scientific limited AD-6   | HP 6890 Series Gas Chromatograph  |
| Measuring items | Density   | Distillation degree  | Octane number<br>Higher heating value<br>Chemical components                          |

## 3. Results and Discussion

Figure 1 illustrates the key physical and chemical properties of the fuels examined in this study. In Figure 1a, the octane numbers of the tested fuels are displayed, comprising both the Research Octane Number (RON) and Motor Octane Number (MON). Both the terms RON and MON refer to a fuel's resistance to detonation under compression within an ICE. RON primarily characterizes the fuel's performance under low-

temperature and low-speed conditions, while MON focuses on its performance under high-temperature and high-speed conditions [33]. It is noteworthy that the MON values for the tested fuels are 9 to 18 units lower than their respective RON values, except for bio-naphtha. Bio-naphtha exhibits similar RON and MON values, which aligns with previous reports [34]. This can be attributed to the high paraffin content in Naphtha. Fuels with a higher proportion of non-paraffin components tend to display a greater disparity between RON and MON values [35]. EtG and G40 were designed to emulate conventional gasoline. The RON and MON values of EtG closely resemble those of gasoline, whereas G40 exhibits higher values compared to gasoline.

In Figure 1b, the Higher Heating Value (HHV) of the tested fuels is depicted. The HHV represents the total heat released during complete combustion of a fuel. The results indicate that EtG, G40, and bio-naphtha possess HHV values similar to that of gasoline. However, DMC exhibits an HHV approximately 35% of that of gasoline, whereas Bioethanol exhibits approximately 65% of gasoline’s HHV. The HHV results suggest that, theoretically, the injection duration of DMC should be three times longer than that of gasoline to deliver the same amount of fuel energy. However, an extended injection duration may lead to isochoric combustion, which compromises engine combustion efficiency. Consequently, alternative approaches such as incorporating additional injector holes, increasing injector hole diameters, or raising injection pressures should be considered when utilizing DMC. On the other hand, similar injection strategies can be employed when adopting EtG, G40, and bio-naphtha in a gasoline engine.

Figure 1c displays the fuel densities of the tested fuels. The densities of EtG, G40, and bio-naphtha closely resemble that of gasoline, while DMC and Bioethanol exhibit a density of approximately 147% and 109% of that of gasoline’s density, respectively. Fuel density plays a crucial role in spray characteristics and subsequent combustion processes in internal combustion engines (ICEs). Higher fuel density typically leads to a narrower spray cone angle [36], the formation of larger droplets [37], longer ignition delays, and slower flame speeds [38].

In Figure 1d, the distillation degree of the tested fuels is presented. The distillation degree, also referred to as the boiling range, represents the temperature range at which different fractions or components within the fuel vaporize [39]. Pure substances like DMC and bioethanol fully vaporize at specific temperatures, namely 88 °C and 78 °C, respectively. Gasoline, EtG, G40, and bio-naphtha, however, require temperatures exceeding 200 °C for complete volatilization. It has been reported that fuels with narrower distillation ranges exhibit a more uniform composition, resulting in improved spray atomization and combustion characteristics. Conversely, fuels with wider distillation ranges may experience uneven vaporization, leading to issues such as fuel droplet breakup or incomplete combustion [40]. Based on this assumption, bio-Naphtha may exhibit a better-performing spray characteristics compared to gasoline, EtG and G40 under evaporative conditions.

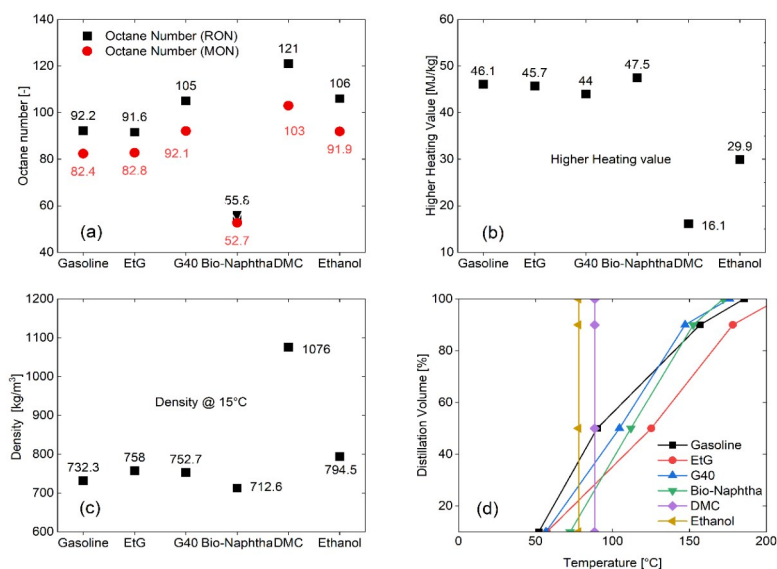


**Figure 1.** Key physical and chemical properties of the tested fuels: (a) Research Octane Number (RON) and Motor Octane Number (MON) values; (b) Higher Heating Value; (c) fuel densities; (d) distillation volume degrees.

The distillation volume degrees of the DMC and bioethanol blends with gasoline were subjected to detailed analysis, as depicted in Figure 2. The data presented in the figures unveil a non-linear correlation between the distillation volume degrees and the blending ratio. At an 80% blend ratio, the distillation speed simply equals the sum of individual rates. However, at a 60% blend ratio, gasoline distillation accelerates initially, until DMC or bioethanol completely evaporates, after which gasoline distillation returns to its normal rate. The specific reasons behind these behaviors are not definitively understood. One potential explanation is the possibility of azeotropic behavior. Azeotropic behavior can significantly influence the distillation rates and characteristics of fuel blends, leading to deviations from the expected linear relationship between composition and distillation rate [41]. In the case of blending DMC with gasoline, and ethanol with gasoline, the observed behaviors could indeed be indicative of the presence of azeotropic mixtures at certain blend ratios. However, further investigation and analysis would be necessary to confirm the presence and impact of azeotropic behavior in these systems. On the other hand, these findings suggest that the spray characteristics and combustion behavior of DMC and bioethanol blends may exhibit substantial variations when the blending ratio exceeds 60%, thereby warranting further in-depth investigations.

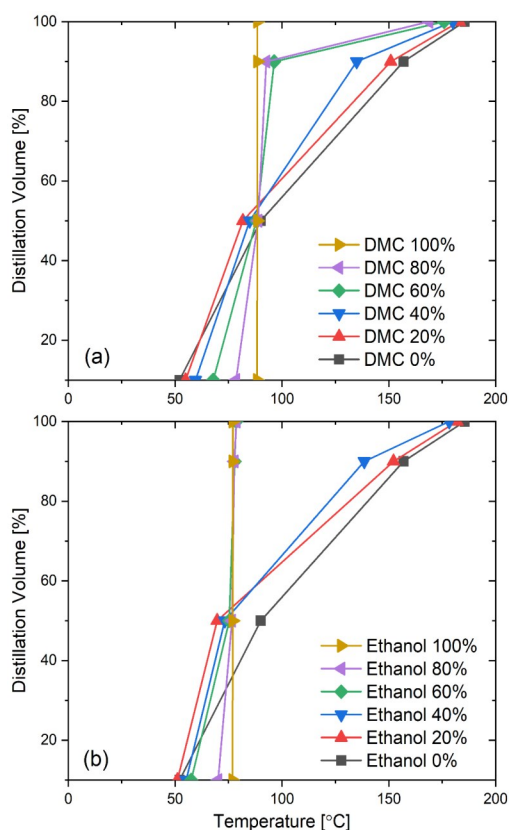


**Figure 2.** Distillation volume degrees of the blends of (a) DMC (dimethyl carbonate) and (b) bioethanol with gasoline.

The impact of chemical compositions on fuel properties, spray characteristics, and combustion behavior is a subject of considerable importance [42–44]. Figure 3 shows the chemical compositions of gasoline, G40, EtG and bio-naphtha.

The results indicate that, in comparison to gasoline, EtG exhibits notably higher proportions of aromatics, as depicted in Figure 1. This difference may account for the higher fuel density observed in EtG when compared to gasoline. This correlation is supported by the findings of Elmalik et al. [42], who reported a robust linear relationship between density and the content of cyclo-paraffins. Aromatics, which are cyclic hydrocarbons with conjugated double bonds, tend to exhibit a lower laminar burning velocity [45], higher tendency for particle mass (PM) and particle number (PN) emissions [46].

On the other hand, G40 demonstrates a relatively higher proportion of iso-paraffins in comparison to gasoline and EtG. Study has indicated that an increased concentration of iso-paraffins tends to raise the

octane rating and enhance the fuel's resistance to knocking [47]. Therefore, the larger RON and MON of G40, as compared to gasoline and EtG, can be attributed to this higher iso-paraffin content. It should be noted that G40 is composed of 10% bioethanol and 30% MtG, combined with 60% gasoline in volumetric fraction. Ethanol is known to possess a higher RON/MON than regular gasoline, as demonstrated in Figure 1a. However, it is argued that the primary driver behind the higher RON/MON of G40 is not because of the ethanol fraction, as a 10% ethanol content alone would not significantly affect the RON/MON. Subsequent sections will provide further evidence to support this argument.

Bio-naphtha stands out with its elevated fraction of paraffin and naphthene components in relation to other synthetic fuels. It is well-documented that fuels characterized by a higher proportion of paraffin constituents often exhibit similar RON and MON values [34]. Naphthenes, which are cyclic hydrocarbons with saturated rings, can influence the volatility and viscosity of fuels [48]. Consequently, the narrower distillation range observed in bio-naphtha can enhance spray atomization and combustion characteristics, as shown in Figure 1. Notably, bio-naphtha showcases an extremely low fraction of aromatics, amounting to only 3.13%. Bio-naphtha possesses considerably small fractions of aromatics, which should account for the lower RON/MON of bio-naphtha compared to gasoline. Moreover, as mentioned earlier, research has indicated that aromatics tend to induce the formation of PM and PN. As a result, bio-naphtha should be able to avoid the formation of PM and PN emissions due to the fuel property nature.

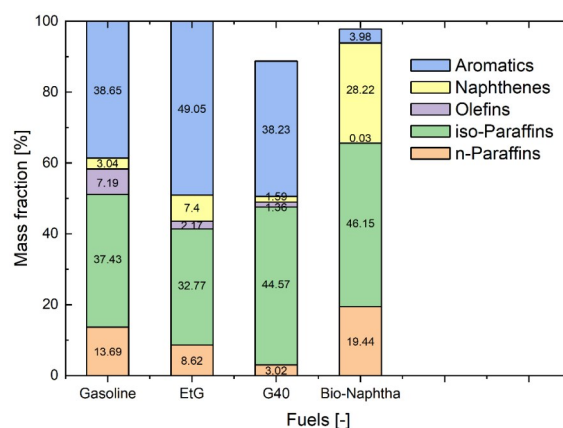


**Figure 3.** Chemical compositions of gasoline, G40, EtG (ethanol-to-gasoline) and bio-naphtha.

The chemical compositions, categorized based on varying carbon atom numbers, have been subjected to a comprehensive analysis, as illustrated in Figure 4. A noteworthy distinction between gasoline and EtG is the higher content of C8 and C10 aromatics in EtG. Extensive studies have revealed that heavy aromatics ( $C \geq 9$ ) have a more significant impact on particle number (PN) emissions than the total aromatic content [49].

G40 exhibits a notable fraction of C8 iso-paraffins. A well-known example of a C8 iso-paraffin is 2,2,4-trimethylpentane, commonly referred to as iso-octane. While it is difficult to ascertain whether the C8 iso-paraffin in G40 corresponds specifically to iso-octane or other compounds, the higher concentration of iso-paraffins in G40 is likely responsible for its greater RON and MON relative to gasoline and EtG. Furthermore, G40 has a higher proportion of C8 iso-paraffins and aromatics compared to gasoline, which contains a greater proportion of lighter carbon compounds. This compositional difference likely contributes to the higher fuel density observed in G40.

Bio-naphtha encompasses carbon chains ranging from 5 to 10 carbon atoms. It possesses a relatively larger share of naphthenes with 7 and 8 carbon atoms, specifically cycloheptane and cyclooctane. Studies have indicated that naphthenes may contribute to PN emissions similar to aromatics [50]. It is noticed that bio-naphtha account only 0.03% of olefin, much less than gasoline. According to reports, while olefins enhance gasoline performance by improving reactivity and anti-knock properties, their impact on emissions varies depending on factors like molecular structure and engine technology [51].

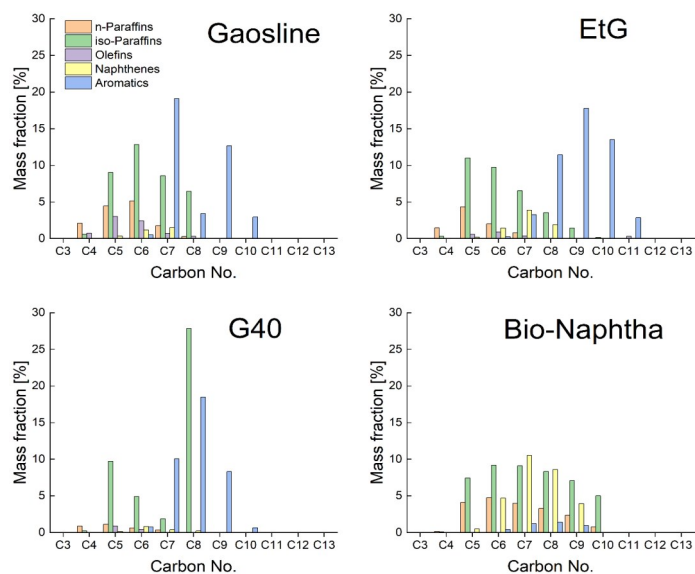


Figure 4. Chemical compositions categorized by carbon atoms number of gasoline, G40, EtG and bio-naphtha.

Figure 5 presents the chemical compositions (Figure 5a) and the RON value and HHV (Figure 5b) of blends consisting of bioethanol and gasoline. Pure ethanol does not possess paraffins, olefins, naphthenes, and aromatics. As the volumetric fraction of ethanol increases in the blends, both the chemical compositions and the RON/HHV demonstrate a predominantly linear change. The investigation of ethanol blends in gasoline has been extensively conducted. The addition of ethanol to gasoline has been found to enhance the laminar flame speed, as reported in [52]. Moreover, studies have indicated an increase in engine brake power and torque with lower ethanol proportions (5–20%), while higher proportions result in a notable rise in brake specific fuel consumption [30].

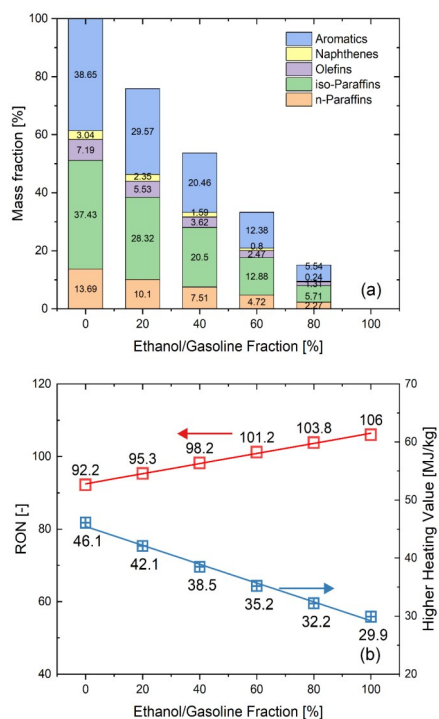


Figure 5. Chemical compositions (a) and the RON/HHV (higher heating value) (b) of the blends of bioethanol with gasoline.



#### 4. Conclusions

Synthetic fuels have garnered significant attention due to their promising characteristics. A comprehensive survey of synthetic fuels available in the global market has been conducted. Subsequently, an investigation was conducted to assess the potential of current synthetic fuels in engines. This report presents preliminary results on the physical and chemical properties of synthetic gasoline-like fuels, namely DMC (dimethyl carbonate), bioethanol, EtG (ethanol-to-gasoline), G40, and bio-naphtha. A comparison is made between these synthetic fuels and conventional gasoline, accompanied by discussions to provide further insights into the potential impact of fuel properties on spray and combustion characteristics. The key findings of the study are summarized below:

(1) EtG is specifically designed to emulate conventional gasoline. It possesses identical research octane number (RON), motor octane number (MON), fuel density, and higher heating value (HHV) as gasoline. However, a notably higher fractions of aromatics was observed in EtG, which may result in a lower laminar burning velocity and higher tendency for particle mass (PM) and particle number (PN) emissions compared to gasoline.

(2) G40 is also engineered to emulate conventional gasoline. It exhibits identical fuel density and HHV as gasoline. However, G40 possesses a higher RON (105) compared to gasoline (92.2), likely attributable to its elevated content of iso-paraffins.

(3) Bio-naphtha, used in this study, contains carbon chains ranging from 5 to 10 carbon atoms. It exhibits a relatively high fraction of paraffins and naphthenes, while its aromatic content is considerably low compared to other fuels. Consequently, bio-naphtha exhibits a lower RON (55.9), lower HHV, and smaller fuel density relative to other synthetic fuels.

(4) Blends of DMC and bioethanol with gasoline were investigated. The data unveil a non-linear correlation between the distillation degrees and the blending ratio. Under a 60% blend ratio, gasoline distillation accelerates initially, until DMC or bioethanol completely evaporates, after which gasoline distillation returns to its normal rate. With an increase in the volumetric fraction of ethanol in the blends, there is a linear change observed in both the chemical compositions and the RON/HHV.

**Author Contributions:** Conceptualization, W.H., K.K., M.O. and K.T.; methodology, W.H., K.K., Y.A., M.O. and K.T.; software, Y.A.; validation, Y.A. and W.H.; formal analysis, Y.A.; investigation, W.H.; resources, K.K. and M.O.; data curation, Y.A. and W.H.; writing—original draft preparation, W.H.; writing—review and editing, K.K., M.O. and K.T.; visualization, Y.A. and W.H.; supervision, M.O.; project administration, M.O.; funding acquisition, M.O. All authors have read and agreed to the published version of the manuscript.

**Funding:** This research was funded by Research on Carbon Recycling and Next-Generation Thermal Power Generation Technologies, CO<sub>2</sub> Emission Reduction and Utilization Technologies, CO<sub>2</sub> Utilization Technologies for Liquid Fuels, and Next-Generation FT Reaction and Integrated Process for Liquid Synthetic Fuel Production of New Energy and Industrial Technology Development Organization (NEDO).

**Data Availability Statement:** Not applicable.

**Acknowledgments:** This research is one of the projects promoted by NEDO, managed by JPEC as a leader of the fuel utilizing working group of the NEDO project. The authors appreciate the financial support from NEDO, and the research collaboration with JPEC.

**Conflicts of Interest:** The authors declare no conflict of interest.

#### References

1. Alamia, A.; Magnusson, I.; Johnsson, F.; Thunman, H. Well-to-wheel analysis of bio-methane via gasification, in heavy duty engines within the transport sector of the European Union. *Appl. Energy* **2016**, *170*, 445–454. <https://doi.org/10.1016/J.APENERGY.2016.02.001>.
2. Hombach, L. E.; Doré, L.; Heidgen, K.; Maas, H.; Wallington, T. J.; Walther, G. *Economic and environmental assessment of current (2015) and future (2030) use of E-fuels in light-duty vehicles in Germany. J. Cleaner Prod.* **2019**, *207*, 153–162. <https://doi.org/10.1016/j.jclepro.2018.09.261>.
3. Garcia, A.; Monsalve-Serrano, J.; Villalta, D.; Tripathi, S. Electric Vehicles vs E-fuelled ICE Vehicles: Comparison of potentials for life cycle CO<sub>2</sub> emission reduction (No. 2022-01-0745). WCX SAE World Congress Experience. *SAE Tech. Pap.* **2022**, 1–15. <https://doi.org/10.4271/2022-01-0745>.
4. Exclusive: EU drafts plan to allow e-fuel combustion engine cars|Reuters n.d. Available online: <https://www.reuters.com/business/autos-transportation/eu-proposes-exception-e-fuel-combustion-engines-2035-2023-03-21/> (accessed on 24 May 2023).

5. Japan to advance commercial launch of e-fuel to 2030 from 2040: METI|S&P Global Commodity Insights n.d. Available online: <https://www.spglobal.com/commodityinsights/en/market-insights/latest-news/energy-transition/051623-japan-to-advance-commercial-launch-of-e-fuel-to-2030-from-2040-meti> (accessed on 24 May 2023).
6. Ram, V.; Salkuti, S.R. An Overview of Major Synthetic Fuels. *Energies* **2023**, *16*, 2834. <https://doi.org/10.3390/en16062834>.
7. Arvidsson, R.; Persson, S.; Fröling, M.; Svanström, M. Life cycle assessment of hydrotreated vegetable oil from rape, oil palm and Jatropha. *J. Cleaner Prod.* **2011**, *19*, 129–137. <https://doi.org/10.1016/j.jclepro.2010.02.008>.
8. Aditiya, H.B.; Mahlia, T.M.I.; Chong, W.T.; Nur, H.; Sebayang, A.H. Second generation bioethanol production: A critical review. *Renewable Sustainable Energy Rev.* **2016**, *66*, 631–653. <https://doi.org/10.1016/j.rser.2016.07.015>.
9. SGS INSPIRE|Europe: HVO 100 available in eight European countries n.d. Available online: <https://inspire.sgs.com/news/102941/europe--pure-hvo-available-in-nine-european-countries> (accessed on 29 May 2023).
10. Ayodele, B.V.; Alsaffar, M.A.; Mustapa, S.I. An overview of integration opportunities for sustainable bioethanol production from first- and second-generation sugar-based feedstocks. *J. Clean. Prod.* **2020**, *245*, 118857. <https://doi.org/10.1016/j.jclepro.2019.118857>.
11. Dahmen, N.; Sauer, J. Evaluation of Techno-Economic Studies on the bioliq<sup>®</sup> Process for Synthetic Fuels Production from Biomass. *Processes* **2021**, *9*, 684. <https://doi.org/10.3390/PR9040684>.
12. Dawood, F.; Anda, M.; Shafiullah, G.M. Hydrogen production for energy: An overview. *Int. J. Hydrogen Energy* **2020**, *45*, 3847–3869. <https://doi.org/10.1016/j.ijhydene.2019.12.059>.
13. Ail, S.S.; Dasappa, S. Biomass to liquid transportation fuel via Fischer Tropsch synthesis—Technology review and current scenario. *Renewable Sustainable Energy Rev.* **2016**, *58*, 267–286. <https://doi.org/10.1016/j.rser.2015.12.143>.
14. Panzone, C.; Philippe, R.; Chappaz, A.; Fongarland, P.; Bengaouer, A. Power-to-Liquid catalytic CO<sub>2</sub> valorization into fuels and chemicals: Focus on the Fischer-Tropsch route. *J. CO<sub>2</sub> Util.* **2020**, *38*, 314–347. <https://doi.org/10.1016/j.jcou.2020.02.009>.
15. Aziz, M.; TriWijayanta, A.; Nandiyanto, A.B.D. Ammonia as effective hydrogen storage: A review on production, storage and utilization. *Energies* **2020**, *13*, 3062. <https://doi.org/10.3390/en13123062>.
16. Dieterich, V.; Buttler, A.; Hanel, A.; Spliethoff, H.; Fendt, S. Power-to-liquid via synthesis of methanol, DME or Fischer—Tropsch-fuels: A review. *Energy Environ. Sci.* **2020**, *13*, 3207–3252. <https://doi.org/10.1039/d0ee01187h>.
17. Staples, M.D.; Isaacs, S.A.; Allroggen, F.; Mallapragada, D.S.; Falter, C.P.; Barrett, S.R.H. Environmental and economic performance of hybrid power-to- liquid and biomass-to-liquid fuel production in the united states. *Environ. Sci. Technol.* **2021**, *55*, 8247–8257. <https://doi.org/10.1021/acs.est.0c07674>.
18. Zhao, J.; Yu, Y.; Ren, H.; Makowski, M.; Granat, J.; Nahorski, Z.; Ma, T. How the power-to-liquid technology can contribute to reaching carbon neutrality of the China’s transportation sector? *Energy* **2022**, *261*, 125058. <https://doi.org/10.1016/J.ENERGY.2022.125058>.
19. Research and development of integrated manufacturing process technology for liquid synthetic fuel from CO<sub>2</sub> (in Japanese). NEDO n.d. Available online: [https://www.nedo.go.jp/news/press/AA5\\_101410.html](https://www.nedo.go.jp/news/press/AA5_101410.html) (accessed on 31 May 2023).
20. Yue, L.; Li, G.; He, G.; Guo, Y.; Xu, L.; Fang, W. Impacts of hydrogen to carbon ratio (H/C) on fundamental properties and supercritical cracking performance of hydrocarbon fuels. *Chem. Eng. J.* **2016**, *283*, 1216–1223. <https://doi.org/10.1016/j.cej.2015.08.081>.
21. Huang, W.; Moon, S.; Ohsawa, K. Near-nozzle dynamics of diesel spray under varied needle lifts and its prediction using analytical model. *Fuel* **2016**, *180*, 292–300. <https://doi.org/10.1016/j.fuel.2016.04.042>.
22. Huang, W.; Moon, S.; Gao, Y.; Li, Z.; Wang, J. Eccentric needle motion effect on near-nozzle dynamics of diesel spray. *Fuel* **2017**, *206*, 409–419. <https://doi.org/10.1016/j.fuel.2017.06.012>.
23. Gao, Y.; Huang, W.; Pratama, R.H.; Wang, J. Transient Nozzle-Exit Velocity Profile in Diesel Spray and Its Influencing Parameters. *Int. J. Automot. Manuf. Mater.* **2022**, *1*, 8.
24. Gao, Y.; Huang, W.; Pratama, R.H.; Gong, H.; Wang, J. Investigation of Needle Motion Profile Effect on Diesel Spray in Near-Nozzle Field. *Micromachines* **2022**, *13*, 1944. <https://doi.org/10.3390/mi13111944>.
25. Zhai, C.; Zhang, G.; Jin, Y.; Nishida, K.; Ogata, Y.; Luo, H. Characterization of diesel spray combustion using two-color pyrometry and OH\* chemiluminescence imaging—Comparison between micro-hole and ultra-high injection pressure effects. *J. Energy Inst.* **2022**, *103*, 104–116. <https://doi.org/10.1016/j.joei.2022.05.012>.
26. Zhai, C.; Liu, E.; Zhang, G.; Xing, W.; Chang, F.; Jin, Y.; Luo, H.; Nishida, K.; Ogata, Y. Similarity and normalization study of fuel spray and combustion under ultra-high injection pressure and micro-hole diameter conditions—spray characteristics. *Energy* **2024**, *288*, 129684. <https://doi.org/10.1016/j.energy.2023.129684>.
27. Toedter, O. *Renewable Fuels ReFuels as Necessary Component for a GHG Neutral Mobility*; Institute of Technology Karlsruhe: Karlsruhe, Germany, 2022.
28. Glossary—What are the different types of sustainable fuels?|Coryton n.d. Available online: <https://coryton.com/lab/articles/glossary-what-are-the-different-types-of-sustainable-fuels/> (accessed on 1 June 2023).
29. Abdalla, A.O.G.; Liu, D. Dimethyl carbonate as a promising oxygenated fuel for combustion: A review. *Energies* **2018**, *11*, 1552. <https://doi.org/10.3390/en11061552>.
30. Thakur, A.K.; Kaviti, A.K.; Mehra, R.; Mer, K.K.S. Progress in performance analysis of ethanol-gasoline blends on SI engine. *Renewable Sustainable Energy Rev.* **2017**, *69*, 324–340. <https://doi.org/10.1016/j.rser.2016.11.056>.
31. Hennig, M.; Haase, M. Techno-economic analysis of hydrogen enhanced methanol to gasoline process from biomass-derived synthesis gas. *Fuel Process. Technol.* **2021**, *216*, 106776. <https://doi.org/10.1016/j.fuproc.2021.106776>.
32. Gas Chromatography Fundamentals n.d. Available online: <https://www.agilent.com/en/product/gas-chromatography/>

- what-is-gas-chromatography (accessed on 22 August 2023).
33. Octane rating—Wikipedia n.d. Available online: [https://en.wikipedia.org/wiki/Octane\\_rating](https://en.wikipedia.org/wiki/Octane_rating) (accessed on 6 June 2023).
  34. Xing, T.; De Crisci, A.G.; Chen, J. Hydrocracking of Fischer-Tropsch wax and its mixtures with heavy vacuum gas oil. *Can. J. Chem. Eng.* **2019**, *97*, 1515–1524. <https://doi.org/10.1002/cjce.23367>.
  35. Javed, T.; Nasir, E.F.; Ahmed, A.; Badra, J.; Djebbi, K.; Beshir, M.; Ji, W.; Sarathy, S.M.; Farooq, A. Ignition delay measurements of light naphtha: A fully blended low octane fuel. *Proc. Combust. Inst.* **2017**, *36*, 315–322. <https://doi.org/10.1016/j.proci.2016.05.043>.
  36. Pratama, R.H.; Huang, W.; Moon, S. Unveiling needle lift dependence on near-nozzle spray dynamics of diesel injector. *Fuel* **2021**, *285*, 119088. <https://doi.org/10.1016/j.fuel.2020.119088>.
  37. Huang, W.; Pratama, R.H.; Oguma, M.; Kinoshita, K.; Takeda, Y.; Suzuki, S. Spray dynamics of synthetic dimethyl carbonate and its blends with gasoline. *Fuel* **2023**, *341*, 127696. <https://doi.org/10.1016/j.fuel.2023.127696>.
  38. Liu, H.; Ma, J.; Dong, F.; Yang, Y.; Liu, X.; Ma, G.; Zheng, Z.; Yao, M. Experimental investigation of the effects of diesel fuel properties on combustion and emissions on a multi-cylinder heavy-duty diesel engine. *Energy Convers. Manag.* **2018**, *171*, 1787–1800. <https://doi.org/10.1016/j.enconman.2018.06.089>.
  39. Distillation—Wikipedia n.d. Available online: <https://en.wikipedia.org/wiki/Distillation> (accessed on 5 June 2023).
  40. Siebers, D.L. Liquid-Phase Fuel Penetration in Diesel Sprays. *SAE Trans.* **1998**, *107*, 1205–1227.
  41. Andersen, V.F.; Anderson, J.E.; Wallington, T.J.; Mueller, S.A.; Nielsen, O.J. Distillation Curves for Alcohol—Gasoline Blends. *Energy Fuels* **2010**, *24*, 2683–2691. <https://doi.org/10.1021/ef9014795>.
  42. Elmalik, E.E.; Raza, B.; Warrag, S.; Ramadhan, H.; Alborzi, E.; Elbashir, N.O. Role of hydrocarbon building blocks on gas-to-liquid derived synthetic jet fuel characteristics. *Ind. Eng. Chem. Res.* **2014**, *53*, 1856–1865. <https://doi.org/10.1021/ie402486c>.
  43. Huang, W.; Moon, S.; Wang, J.; Murayama, K.; Arima, T.; Sasaki, Y.; Arioka, A. Nozzle tip wetting in gasoline direct injection injector and its link with nozzle internal flow. *Int. J. Engine Res.* **2019**, *21*, 340–351. <https://doi.org/10.1177/1468087419869774>.
  44. Huang, W.; Gong, H.; Moon, S.; Wang, J.; Murayama, K.; Taniguchi, H.; Arima, T.; Arioka, A.; Sasaki, Y. Nozzle Tip Wetting in GDI Injector at Flash-boiling Conditions. *Int. J. Heat Mass Transf.* **2021**, *169*, 120935. <https://doi.org/10.1016/j.ijheatmasstransfer.2021.120935>.
  45. Farrell, J.T.; Johnston, R.J.; Androulakis, I.P. Molecular structure effects on laminar burning velocities at elevated temperature and pressure. *SAE Tech. Pap. SAE Int.* **2004**, *113*, 1404–1425. <https://doi.org/10.4271/2004-01-2936>.
  46. Zhang, W.; Ma, X.; Shuai, S.; Wu, K.; Macias, J.R.; Shen, Y.; Yang, C.; Guan, L. Effect of gasoline aromatic compositions coupled with single and double injection strategy on GDI engine combustion and emissions. *Fuel* **2020**, *278*, 118308. <https://doi.org/10.1016/j.fuel.2020.118308>.
  47. Briker, Y.; Ring, Z. Diesel fuel analysis by GC-FIMS: Aromatics, n-paraffins, and isoparaffins. *Energy Fuels* **2001**, *15*, 23–37. <https://doi.org/10.1021/ef000106f>.
  48. Schifter, I.; González, U.; Díaz, L.; Sánchez-Reyna, G.; Mejía-Centeno, I.; González-Macías, C. Comparison of performance and emissions for gasoline-oxygenated blends up to 20 percent oxygen and implications for combustion on a spark-ignited engine. *Fuel* **2017**, *208*, 673–681. <https://doi.org/10.1016/j.fuel.2017.07.065>.
  49. Zhang, W.; Ma, X.; Shuai, S.; Wu, K.; Macias, J.R.; Shen, Y.; Yang, C.; Guan, L. Effect of gasoline aromatic compositions coupled with single and double injection strategy on GDI engine combustion and emissions. *Fuel* **2020**, *278*, 118308. <https://doi.org/10.1016/j.fuel.2020.118308>.
  50. Li, Z.; Liu, G.; Cui, X.; Sun, X.; Li, S.; Qian, Y.; Jiang, C.; Lu, X. Effects of the variation in diesel fuel components on the particulate matter and unregulated gaseous emissions from a common rail diesel engine. *Fuel* **2018**, *232*, 279–289. <https://doi.org/10.1016/j.fuel.2018.05.170>.
  51. Dagle, V.L.; Affandy, M.; Saavedra Lopez, J.; Cosimbescu, L.; Gaspar, D.J.; Goldsborough, S.S.; Rockstroh, T.; Cheng, S.; Han, T.; Kolodziej, C.P.; et al. Production, fuel properties and combustion testing of an iso-olefins blendstock for modern vehicles. *Fuel* **2021**, *310*, 122314. <https://doi.org/10.1016/j.fuel.2021.122314>.
  52. Del Pecchia, M.; Pessina, V.; Berni, F.; d’Adamo, A.; Fontanesi, S. Gasoline-ethanol blend formulation to mimic laminar flame speed and auto-ignition quality in automotive engines. *Fuel* **2020**, *264*, 116741. <https://doi.org/10.1016/J.FUEL.2019.116741>.